Physica B xxx (xxxx) xxx–xxx

Contents lists available at ScienceDirect

Physica B

journal homepage: www.elsevier.com/locate/physb

Growth of C_{60} thin films on Al_2O_3/NiAl(100) at early stages

S.-C. Hsu[a], C.-H. Liao[a], T.-C. Hung[a], Y.-C. Wu[a], Y.-L. Lai[b], Y.-J. Hsu[b], M.-F. Luo[a,*]

[a] Department of Physics, National Central University, 300 Jhongda Road, Jhongli District, Taoyuan 32001, Taiwan
[b] National Synchrotron Radiation Research Center, 101 Hsin-Ann Road, Hsinchu Science Park, Hsinchu 30076, Taiwan

ARTICLE INFO

Keywords:
C_{60}
Thin film growth
Al_2O_3
NiAl
STM
PES

ABSTRACT

The growth of thin films of C_{60} on Al_2O_3/NiAl(100) at the earliest stage was studied with scanning tunneling microscopy and synchrotron-based photoelectron spectroscopy under ultrahigh-vacuum conditions. C_{60} molecules, deposited from the vapor onto an ordered thin film of Al_2O_3/NiAl(100) at 300 K, nucleated into nanoscale rectangular islands, with their longer sides parallel to direction either [010] or [001] of NiAl. The particular island shape resulted because C_{60} diffused rapidly, and adsorbed and nucleated preferentially on the protrusion stripes of the crystalline Al_2O_3 surface. The monolayer C_{60} film exhibited linear protrusions of height 1–3 Å, due to either the structure of the underlying Al_2O_3 or the lattice mismatch at the boundaries of the coalescing C_{60} islands; such protrusions governed also the growth of the second layer. The second layer of the C_{60} film grew only for a C_{60} coverage >0.60 ML, implying a layer-by-layer growth mode, and also ripened in rectangular shapes. The thin film of C_{60} was thermally stable up to 400 K; above 500 K, the C_{60} islands dissociated and most C_{60} desorbed.

1. Introduction

The novel electronic properties of C_{60}-based materials indicate varied prospective applications in both thin-film devices and solar cells, provided that films of high quality can be produced [1–6]. The growth properties of C_{60} in the thin-film regime, especially at the stages of nucleation and monolayer formation, are important in determining the quality of the thin films. Thin films of C_{60} on various substrates, including metal [7–16], semiconductor [17–20] and insulator surfaces [21–25], have hence been intensively studied. With the recent advancement of nanoscale devices, C_{60} thin films patterned on a nanoscale and via a self-organized approach become desirable [14,23]. To respond to the demand, we studied the growth of thin films of C_{60} on alumina grown on NiAl(100) (denoted as Al_2O_3/NiAl(100)) at the initial stages. The alumina surface is one of the most widely studied oxide surfaces, because of its application in catalysis and devices [26]. The ordered Al_2O_3/NiAl(100) surface was shown to have peculiar linear protrusions resulting from a lattice mismatch between the oxide film and the NiAl substrate [27–31]; the protrusions served as nucleation sites for deposited metals [32–34]. The growth of C_{60} thin films on Al_2O_3/NiAl(100) is expected to be guided and the C_{60} thin films to become thus self-patterned.

This investigation was conducted primarily with scanning tunneling microscopy (STM) and synchrotron-based photoelectron spectroscopy (PES). Both sample preparation and measurements were undertaken under ultrahigh vacuum (UHV) conditions. C_{60} was deposited from the vapor onto Al_2O_3/NiAl(100) at 300 K. Our results showed that the growth was governed by the protrusion stripes on the crystalline Al_2O_3 surface – deposited C_{60} formed nanoscale rectangular islands having their longer sides parallel to the protrusion stripes, the direction either [010] or [001] of NiAl. Such anisotropic growth contrasts with other systems having weak C_{60}-substrate interactions, such as C_{60} on graphite [35–37], for which equiaxial islands are observed and was associated largely with an energetically preferable adsorption and nucleation of C_{60} on the protrusions. The behavior implies that, on the Al_2O_3 film on which uniform protrusion stripes propagate uniquely in only one direction [34], the growth direction of the nanoscale rectangular C_{60} islands can be precisely controlled. The C_{60} thin films grew predominantly through a fashion layer by layer, resembling that on graphite [36], TiO_2 (110) [25] and metal surfaces [15] but contrasting that on a KBr surface [22] on which three-dimensional growth proceeds; the guided growth extended atypically to the second layer: the second layer of the C_{60} islands ripened also in rectangular shapes. The thermal stability of the C_{60} thin films was characterized and is discussed in relation to comparable systems.

2. Experiments

Our experiments were performed in UHV chambers with base pressure 4×10^{-10} Torr. A NiAl(100) sample (MaTeck GmbH) was

* Corresponding author.
E-mail address: mfl28@phy.ncu.edu.tw (M.-F. Luo).

http://dx.doi.org/10.1016/j.physb.2017.03.040
Received 13 December 2016; Received in revised form 26 February 2017; Accepted 25 March 2017

polished to a roughness less than 30 nm and an orientation accuracy better than 0.1°. To obtain a clean surface, the sample underwent alternative cycles of sputtering and subsequent annealing before each experiment. The cleanliness of the sample was monitored with Auger electron spectra, low energy electron diffraction (LEED) and STM. An ultra-thin film of θ-Al_2O_3 was formed on oxidation of a NiAl(100) alloy surface at 1000 K; the formation of Al_2O_3 thin films is described elsewhere [27–30]. To achieve a homogeneous crystalline Al_2O_3 surface with limited amorphous oxide surface [30,33], we refrained from protracted post-oxidation annealing of the oxide films. The grown θ-Al_2O_3 thin film had thickness 0.5–1.0 nm [27,30]. The sample was then quenched to 300 K for vapor deposition of C_{60}. The C_{60} coverage was estimated from the volume of the C_{60} islands observed with a STM.

STM images (recorded with a RHK UHV 300 unit), constant-current topographies, were obtained at 150 K with a sample bias voltage typically 3.0–3.8 V and a tunneling current 0.1–0.2 nA; the STM tip consisted of an electrochemically etched tungsten wire. The PES were recorded at the U5-spectroscopy beamline of Taiwan Light Source in National Synchrotron Radiation Research Center (NSRRC) [38]. The total energy resolution, including effects of the beamline and energy analyzer, was estimated to be near 0.1 eV. The photon energies were fixed at 383 eV throughout these experiments. The beam was incident normal to the surface; photoelectrons were collected at angle 58° from the surface normal. All photoelectron spectra presented here were first normalized to the photon flux. The BE in core-level spectra was referred to the substrate bulk Al 2p core level at 72.9 eV [29,39–41].

3. Results and discussion

We observed the morphological evolution of the Al_2O_3/NiAl(100) surface during the deposition of C_{60} with STM. C_{60} islands formed in an anisotropic manner on the crystalline Al_2O_3 surface; they were mostly rectangular and developed preferentially along directions [010] and [001] of NiAl substrate. Fig. 1(a) exemplifies the STM image for the Al_2O_3/NiAl(100) surface. The oxide surface typically consists of crystalline (marked by *A* in Fig. 1(a)) and amorphous (marked by *B*) areas. The crystalline oxide exhibits protrusion stripes propagating along directions [010] and [001] of NiAl [28,30–33], as indicated in the figure; in contrast, the amorphous area is rough and structureless [28,30,33]. The crystalline oxide was shown to have a θ-Al_2O_3(100) surface, which has a (2×1) surface unit-cell and the *a*-axis parallel to direction either [010] or [001] of NiAl [29,42–44], as schematically illustrated in Fig. 1(b). The protrusions were linear defects induced to release the stress in the Al_2O_3 film, due primarily to the oxide-substrate lattice mismatch (about 2.5%) along the *a*-axis of the (2×1) unit-cell [27,34]. The protrusions thus repeat along the *a*-axis direction [34]; they develop along two directions as the θ-Al_2O_3(100) film grow in two orientations with respect to the substrate [27–33]. In comparison to the perfect (2×1) θ-Al_2O_3(100) surface, the protrusions are likely oxygen deficit, as their electronic structures and chemical properties resemble those on Al_2O_3/NiAl(110) surface [45,46]; they both have increased unoccupied states in the oxide band gap and greater adsorption energy for adsorbates or deposited metals [31–33,45–47], so they seem higher when imaged by STM and they serve as nucleation sites for metals deposited from the vapor [32–34]. The amorphous area in the present study developed largely by partial decomposition of the oxide during post-oxidation annealing; it contains amorphous oxides, bare NiAl(100), and perhaps NiAl nanoclusters [28,30,33,48]. The lateral diffusion of deposited metals or adsorbates is often constrained in the amorphous area [27,28,33]. The area can be reduced by refraining from protracted post-oxidation annealing or repeating oxidation of the surface.

Fig. 2(a)–(d) show STM images of C_{60} at varied coverages (0.1–0.6 ML) on Al_2O_3/NiAl(100) and Fig. 2(e) for C_{60} on NiAl(100) as a comparison. At a small C_{60} coverage (Fig. 2(a)), the crystalline Al_2O_3

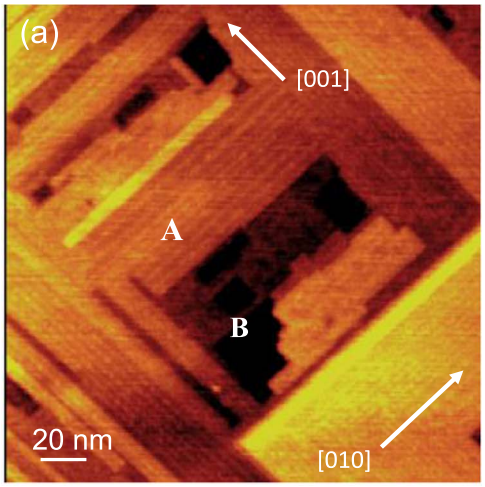

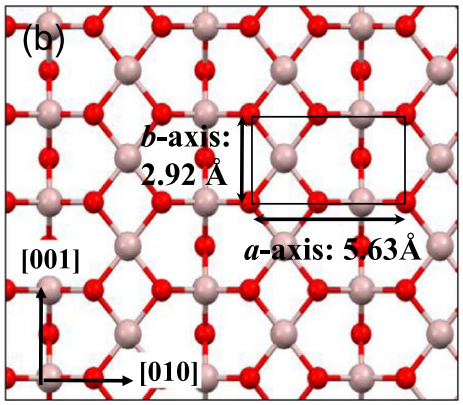

Fig. 1. (a) STM image for the oxidized NiAl(100) surface undergoing 60-min post-oxidation annealing at 1000 K; (b) schematic diagram showing top view for the θ-Al_2O_3(100) surface. The region in (a) marked by A is the crystalline Al_2O_3 and that marked by B is the amorphous area (b) was based on previous DFT calculations and STM images [29,42,43]; the red and grey balls denote O and Al atoms, respectively; the black rectangle indicates the (2×1) surface unit cell. (For interpretation of the references to color in this figure legend, the reader is referred to the web version of this article).

surface is a predominant feature; a few C_{60} islands of height 8–10 Å, demonstrated in lateral profile A in Fig. 2(a), already formed. Notably, the islands were rectangular and had their longer sides parallel to the protrusion stripes, the direction either [010] or [001] of NiAl. At greater C_{60} coverages, the islands grew but exhibited the same structural features (Fig. 2(b)–(d)). The C_{60} molecules in the islands were not resolved because to achieve the resolution requires a reduced sample-STM tip distance, at which the molecules were easily attracted and attached to or pushed around by the scanning tip. In addition to the C_{60} islands, small particles of two kinds, despite being of minor proportion, existed on the surface. The first kind comprised C_{60} molecules adsorbed in the amorphous area of Al_2O_3/NiAl(100), exemplified by the particle chains in the middle (circled) of Fig. 2(a). As the diffusion of C_{60} was restricted in the narrow amorphous area, the C_{60} molecules adsorbed separately, like those adsorbed on a NiAl(100) surface (Fig. 2(e)), and were confined and aligned. The lateral profile across a particle in the amorphous area (B in Fig. 2(a)) shows a full width at half maximum (FWHM) about 10 Å and height about 6 Å; the measured size is the same as that for a single C_{60} molecule on NiAl(100) (Fig. 2(e)) and also near the known size of a C_{60} molecule [49]. The comparison implies that the amorphous area was more like NiAl(100) surface (since the amorphous area contains NiAl facets) and thus that C_{60} molecules were more strongly bound to the amorphous area than to the crystalline Al_2O_3. The other kind is C_{60} adsorbed individually on the crystalline Al_2O_3, observable at varied C_{60} coverage (Fig. 2(a)–(d)). Because of varied tunneling conditions, the